Acta Ciencia Indica, Vol. XLII C, No. 2, 121 (2016)

KINETIC ANALYSIS OF THERMAL DECOMPOSITION OF RUBROCURCUMIN

JEENA JOHN, SUDHA DEVI R., BALACHANDRAN S.

Department of Chemistry, Mahatma Gandhi College, Thiruvananthapuram 695004 (Kerala), India

RECEIVED : 6 June, 2016

Rubrocurcumin, a spiroborate ester of curcumin has been synthesized and characterized by different spectral techniques. The thermogravimetric analysis (TGA) of the complex was carried out for evaluating their decomposition kinetic parameters. The thermal decomposition of rubrocurcumin occurs mainly in four steps and the compound is stable upto 287°C. The TGA data, analyzed using different solid state reaction models, showed that the decomposition can be best described by Mapel first order reaction model. Various differential and integral methods viz., Coats Redfern, Broido, Horowitz-Metzger, Madhusudhanan-Krishnan-Ninan, Freeman-Carrol, Sharp-Wentworth and Achar methods were used in this study for calculating the thermal degradation kinetic parameters and the results are compared and discussed.

INTRODUCTION

Curcumin, a symmetric natural polyphenolic compound, is an active ingredient present in the spice turmeric (Priyadarsini, 2014). The commercial sample of curcumin contains approximately 77% curcumin - C, 17% demethoxycurcumin - DMC and 6% bisdemethoxycurcumin – BDMC (Fig. 1) (Kurien *et al*., 2009). Chemically, curcumin is a bis α, β-unsaturated β-diketone. The β-diketone moiety present in curcumin makes it a powerful chelating agent (Borsari *et al*., 2002). Curcumin has been shown to have many biological activities like antioxidant, anti inflammatory, anti HIV, anti carcinogenic, anti rheumatic activity etc. (Sharma, 1976, Srimal *et al.*, 1973, Jordan *et al*., 1996, Kuttan *et al.*, 1985, Deodhar *et al*., 1980).

Curcumin reacts with stoichiometric amounts of boric acid and oxalic acid to form a red colored dye called rubrocurcumin (Fig. 2) (Balaban *et al*., 2008). The characteristic color change from yellow to red during rubrocurcumin formation is used for the determination of boron in different fields such as nuclear energy, metallurgy, pharmacy and agriculture (Katherine *et al*., 2012). In order to promote the application of rubrocurcumin in medicinal (Sui *et. al.* 1993) and analytical field (Mair and Day, 1972, Baker, 1964), the knowledge of the combustion behaviour and thermodynamic data are useful and essential. TGA can provide idea about the number and sequence of reaction in a thermal decomposition process and theassociated kinetic parameters of these degradation stages. Different kinetic equations were reported in literature for calculating the kinetic parameters and were differ in their complexity and in accuracy of the result (Broido, 1969).

The present work focuses on the thermal stability behaviour of rubrocurcumin to investigate the mechanistic model of the thermal decomposition of rubrocurcumin. The kinetic

parameters, such as the energy of activation (Ea), frequency factor (A), enthalpy change (ΔH), entropy change(ΔS) and free energy change(ΔG) for the main decomposition stages of the complex were calculated using Coats Redfern (CR), Broido (BR), Horowitz-Metzger (HM), Madhusudhanan-Krishnan-Ninan (MKN), Freeman-Carrol (FC), Sharp-Wentworth (SW) and Achar (AC) methods and the results have been compared.

Graphical Abstract

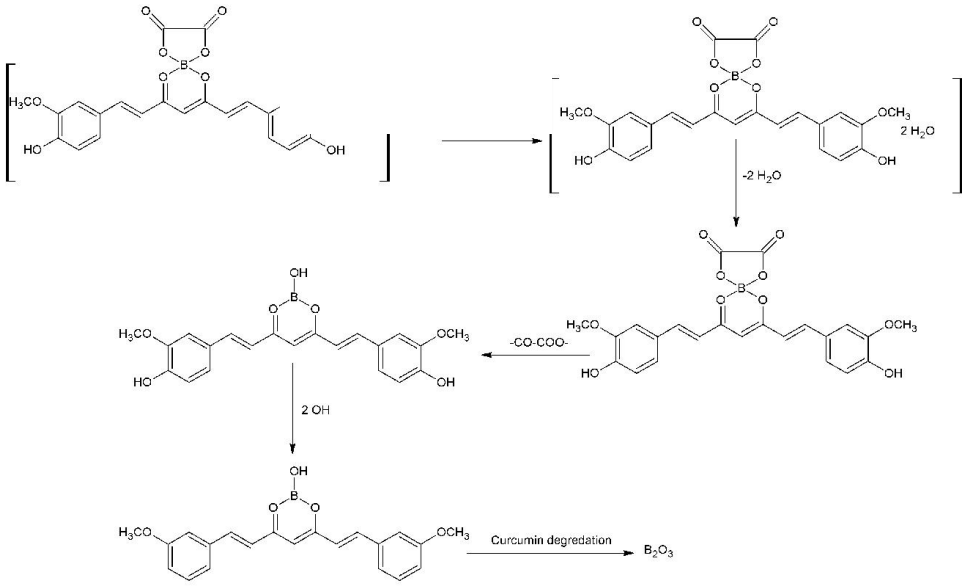

Thermal decomposition steps of rubrocurcumin.

Thermogravimetric analysis of rubrocurcumin has been carried out for evaluating the thermal degradation steps and kinetic parameters associated with these degradation steps. Different mechanistic and non-mechanistic methods have been used for calculating kinetic parameters associated with each stage.

EXPERIMENTAL

Analytical grade oxalic acid and boric acid used for the preparation of rubrocurcumin were obtained from SDS Mumbai. The commercial sample of curcumin was purchased from Merck Chemie Pvt. Ltd. Mumbai. Column chromatography using a column packed with silica gel 60-120 mesh as stationary phase and chloroform as mobile phase were used for the separation of curcumin from DMC and BDMC (Asha *et al*., 2012). Rubrocurcumin was prepared from curcumin using the method reported in literature (Sui *et al*., 1993). The complex was purified and spectral studies were conducted to confirm the structure. Thermal gravimetric analyses were recorded on Perkin-Elmer Thermogravimetric Analyzer. The experiments were carried out in dynamic nitrogen atmosphere (100 mL/min) with a heating rate of 10°C/min in the temperature range of 40-750°C.

The kinetic analyses of the TG - DTG data were carried out using fourteen mechanistic equations and seven non-mechanistic equations. The general equation for the non-isothermal decomposition kinetics of solid state reaction (Henriquea *et al*., 2015, Balogun *et al*., 2014, Flynn, 1983, Ramajo *et al*., 2006) is presented as

$$d\alpha/dT = \frac{A}{\beta} e^{(-Ea/RT)} f(\alpha) \quad \ldots (1)$$

where β is the heating rate (°C min^{-1}), α is the degree of conversion, Ea is the apparent activation energy and A is the pre-exponential factor.

Table 1. Solid state reaction models

Model No.	Name of functions	Rate controlling process	f(α)	g(α)
1	Mampel power law, n =1	Chemical reaction	$1-\alpha$	$-\ln(1-\alpha)$
2	Mampel power law, n = 0	Chemical reaction	1	α
3	Mampel power law, n = 1/3	Chemical reaction	$(1-\alpha)^{1/3}$	$3[1-(1-\alpha)^{1/3}]$
4	Mampel power law, n = 1/2	Chemical reaction	$(1-\alpha)^{1/2}$	$2[1-(1-\alpha)^{1/2}]$
5	Mampel power law, n = 2/3	Chemical reaction	$(1-\alpha)^{2/3}$	$3/2[1-(1-\alpha)^{2/3}]$
6	Mampel power law, n = 2	Chemical reaction	$(1-\alpha)^{2}$	$(1-\alpha)^{-1}-1$
7	Contracting cylinder	Phase boundary reaction symmetry	$2(1-\alpha)^{1/2}$	$[1-(1-\alpha)^{1/2}]$
8	Contracting sphere	Phase boundary reaction spherical symmetry	$3(1-\alpha)^{2/3}$	$[1-(1-\alpha)^{1/3}]$
9	Avrami-Erofeev equation (n = 2)	Assumes random nucleations and its subsequent growth n=2	$2(1-\alpha)[-\ln(1-\alpha)]^{1/2}$	$[-\ln(1-\alpha)]^{1/2}$
10	Avrami-Erofeev equation (n = 3)	Assumes random nucleations and its subsequent growth n=3	$3(1-\alpha)[-\ln(1-\alpha)]^{2/3}$	$[-\ln(1-\alpha)]^{1/3}$
11	Avrami-Erofeev equation (n = 4)	Assumes random nucleations and its subsequent growth n=4	$4(1-\alpha)[-\ln(1-\alpha)]^{3/4}$	$[-\ln(1-\alpha)]^{1/4}$
12	Valensi(Barrer) equation	Two dimensional diffusion and its subsequent growth	$1-\ln(1-\alpha)^{-1}$	$\alpha+(1-\alpha)\ln(1-\alpha)$
13	Jander equation	Three dimensional diffusion	$3/2(1-\alpha)^{2/3}$	$[1-(1-\alpha)^{1/3}]^{2}$
14	Ginstling equation	Three dimensional diffusion spherical symmetry	$3/2[(1-\alpha)^{1/3}-1]^{-1}$	$1-2\alpha/3-(1-\alpha)^{2/3}$

For constant heating rate conditions, integration of equation (1) leads to the equation (2)

$$g(\alpha) = \frac{A}{\beta}\int_0^T e^{(-Ea/RT)}\, dT \quad \ldots (2)$$

The temperature integral can be replaced with various approximations which lead to several non-mechanistic methods for the evaluation of different thermo kinetic parameters. The seven non-mechanistic methods used in this study are

1. CR method

$$\ln\left[\frac{g(\alpha)}{T^2}\right] = \ln\frac{AR}{\beta E}\left[1-\frac{2RT}{E_a}\right]-\frac{E_a}{RT} \quad \ldots (3)$$

Table 2. Results of kinetic analysis using different heterogeneous solid state reaction models.

Model No.	First stage					
	Achar method			Coats Redfern method		
	R^2	Ea (kJ mol^{-1})	A (s^{-1})	R^2	Ea (kJ mol^{-1})	A (s^{-1})
1	0.9922	68.46	2.14×10^{8}	0.9891	65.13	1.23×10^{6}
2	0.9977	51.60	7.68×10^{5}	0.8830	57.33	7.94×10^{4}
3	0.9994	57.22	5.02×10^{6}	0.0230	–1.39	-2.74×10^{-4}
4	0.9982	60.03	1.28×10^{7}	0.6054	2.52	9.30×10^{-4}
5	0.9961	62.84	3.28×10^{7}	0.9877	59.79	1.89×10^{5}
6	0.9666	85.31	5.97×10^{10}	0.9309	74.18	2.86×10^{7}
7	0.9982	60.03	6.41×10^{6}	0.9235	61.08	1.48×10^{5}
8	0.9976	62.84	1.09×10^{7}	0.9484	62.39	1.57×10^{5}
9	0.9895	32.74	3.39×10^{3}	0.9272	29.42	1.75×10^{1}
10	0.9888	20.83	7.14×10^{1}	0.9324	17.51	3.30×10^{-1}
11	0.9882	14.88	9.52×10^{0}	0.9386	11.56	3.87×10^{-2}
12	0.9973	63.68	4.43×10^{7}	0.9191	–10.17	-1.03×10^{-4}
13	0.9961	62.84	2.18×10^{7}	0.9458	131.09	4.39×10^{13}
14	0.9584	120.30	6.83×10^{13}	0.9091	127.54	1.30×10^{13}
Second stage						
	Achar method			Coats Redfern method		
	R^2	Ea (kJ mol^{-1})	A (s^{-1})	R^2	Ea (kJ mol^{-1})	A (s^{-1})
1	0.9967	661.4040	1.22×10^{60}	0.9899	683.20	1.04×10^{61}
2	0.1233	-7.13913	1.11×10^{-1}	0.8837	444.36	5.35×10^{38}
3	0.5520	212.9231	2.47×10^{19}	0.9562	59.15	2.40×10^{3}
4	0.9321	322.9543	3.68×10^{29}	0.9519	105.70	4.70×10^{7}
5	0.9693	432.9855	5.49×10^{39}	0.9250	505.93	3.08×10^{44}
6	0.9494	1313.234	1.35×10^{121}	0.9874	1104.55	1.5×10^{100}
7	0.9047	322.9543	1.84×10^{29}	0.9583	542.74	4.22×10^{47}
8	0.9749	432.9855	1.83×10^{39}	0.9694	584.27	2.11×10^{51}
9	0.9980	306.7049	1.43×10^{28}	0.9862	336.86	1.2×10^{29}
10	0.7637	191.2573	2.72×10^{17}	0.9858	221.41	2.26×10^{18}

11	0.9777	133.5334	1.09×10^{12}	0.9854	163.68	8.93×10^{12}
12	0.5444	411.4930	8.03×10^{36}	0.1943	-12.67	-9.6×10^{-5}
13	0.9749	432.9855	3.66×10^{39}	0.9699	1178.03	1.8×10^{105}
14	0.7663	61.49917	1.20×10^{05}	0.9538	1063.69	4.38×10^{94}

Table 3. Kinetic parameters of rubrocurcumin calculated using different methods.

Stage	Equation due to	R^2	Ea (kJ mol^{-1})	A (s^{-1})	ΔH (kJ mol^{-1})	ΔS (JK^{-1} mol^{-1})	ΔG (kJ mol^{-1})
First	CR	0.989081	65.13	1.23×10^{6}	61.68	– 139.43	119.68
	BR	0.985591	71.44	8.27×10^{6}	67.98	– 123.56	119.38
	MKN	0.989144	65.32	8.47×10^{6}	61.86	– 123.36	113.18
	SW	0.990049	89.28	3.57×10^{7}	85.82	– 111.40	132.16
	AC	0.992232	68.46	2.14×10^{8}	85.82	– 96.51	125.96
	FC	0.991732	78.91	8.54×10^{7}	75.45	– 104.15	118.78
	HM	0.985591	86.19	6.64×10^{8}	82.73	– 87.09	118.96
Second`	CR	0.986645	683.19	1.04×10^{61}	678.47	909.54	160.94
	BR	0.98804	630.62	7.16×10^{61}	625.89	925.55	99.25
	MKN	0.98666	620.89	5.66×10^{61}	616.16	923.59	90.64
	SW	0.991012	653.05	1.05×10^{60}	648.32	890.43	141.66
	AC	0.997799	653.05	1.22×10^{60}	648.32	891.71	140.94
	FC	0.991012	615.92	7.05×10^{60}	611.19	906.27	95.52
	HM	0.991865	687.99	6.17×10^{61}	683.26	924.30	157.33

where $\alpha = \frac{w_0 - w_t}{w_0 - w_t} w_0$ is the initial mass of the sample, w_t is the mass of the sample at temperature T, w_f is the final mass at temperature at which the mass loss is approximately unchanged, g (α) = [– ln (1 – α)] for first order reactions. A plot of $\ln\left[-\frac{\ln(1-\alpha)}{T^2}\right]$ against 1/T was found to be linear. From the slope of this plot, the Ea was calculated. A was calculated from the intercept (Coats and Redfern, 1964).

2. BR method

$$\ln\left[-\ln(1-\alpha)\right] = \frac{-Ea}{RT} + \ln\left[\frac{ART_s^2}{\beta Ea}\right] \quad \ldots (4)$$

where (1 – α) is the fraction of number of initial molecules not yet decomposed, T is the temperature in Kelvin. Plotting ln [– ln (1 – α)] vs. 1/T should result in a straight line, the slope of which can provide the value of Ea (Broido, 1969).

3. MKN method

$$\ln\frac{g(\alpha)}{T^{1.9206}} = \ln\left(\frac{AEa}{\beta R}\right) + 3.7678 - 1.9206\ \ln Ea - 0.12040\left({}^{Ea}/_{T}\right) \quad \ldots (5)$$

The plot of LHS of the above equation versus 1/T give linear curve and Ea and A are calculated from the slope and intercept (Madhusudhanan *et al*., 1986).

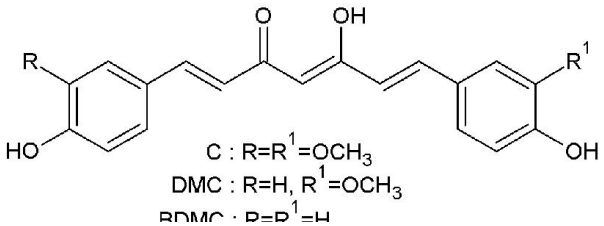

Fig. 1. Chemical structure of curcuminoids.

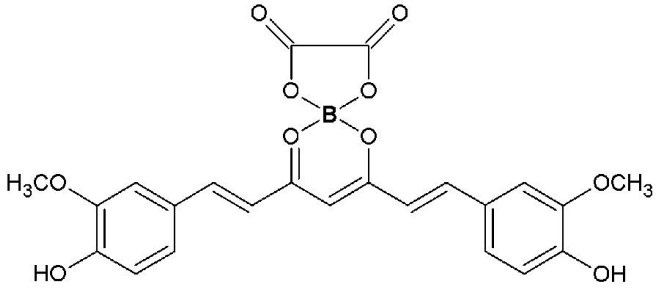

Fig. 2. Chemical structure of rubrocurcumin.

4. SW method

$$\ln\left[\frac{\left(dc/dt\right)}{(1-c)}\right] = \ln\left(A/\beta\right) - \left[Ea/RT\right] \quad \ldots (6)$$

where $\frac{dc}{dt}$ is the rate of change of fraction of weight with change in temperature. By plotting a graph between $\ln\left[\frac{(dc/dt)}{(1-c)}\right]$ versus 1/T should be a straight line which gives Ea from its slope (Sharp and Wentworth, 1969).

5. FC method

$$\ln\left[\frac{dw/dt}{W_r}\right] = \ln A - \frac{Ea}{RT} \quad \ldots (7)$$

where $\frac{dw}{dt}$ is the rate of change of weight with time, $w_r = w_c - w$ and w is the fraction of weight loss at time t and w_c is the weight loss at the completion of the reaction. By plotting the graph between $\ln\left[\frac{dw/dt}{w_r}\right]$ versus 1/T should be a straight line for decomposition following first order kinetics with a slope of $\left(-\frac{Ea}{R}\right)$ and A was obtained from the intercept on former axis (Freeman and Carrol, 1958).

6. HM method

$$\ln\ln\left(\frac{w_0}{w_t}\right) = \frac{Ea\theta}{RT_s^2} \quad \ldots (8)$$

where $\theta = T - T_s$, T is the temperature at particular weight loss, Ts is the peak temperature, w_o is the initial weight and w_t is the weight at any time. A plot of $lnln\left({}^{w_0}/_{w_t}\right)$ versus θ gives an excellent approximation to a straight line. From the slope activation energy can be calculated. The frequency factor, A, is calculated using equation (9) (Horowitz and Metzger, 1963).

$$\frac{\mathrm{Ea}}{\mathrm{RT}^2} = \frac{\mathrm{A}}{\beta \mathrm{e}^{-\mathrm{Ea}/\mathrm{RT_s}}} \quad \ldots (9)$$

Achar method

$$\ln\left[\frac{\mathrm{d}\alpha/\mathrm{dt}}{\mathrm{f}(\alpha)}\right] = \ln\mathrm{A} - \frac{\mathrm{Ea}}{\mathrm{RT}} \quad \ldots (10)$$

where $d\alpha/dt$ is the rate of conversion, f (α) is the differential mechanism function. A plot of $\ln\left[\frac{d\alpha/dt}{f(\alpha)}\right]$ versus 1/T is a straight line from which the Ea and A were calculated (Achar *et al*., 1966).

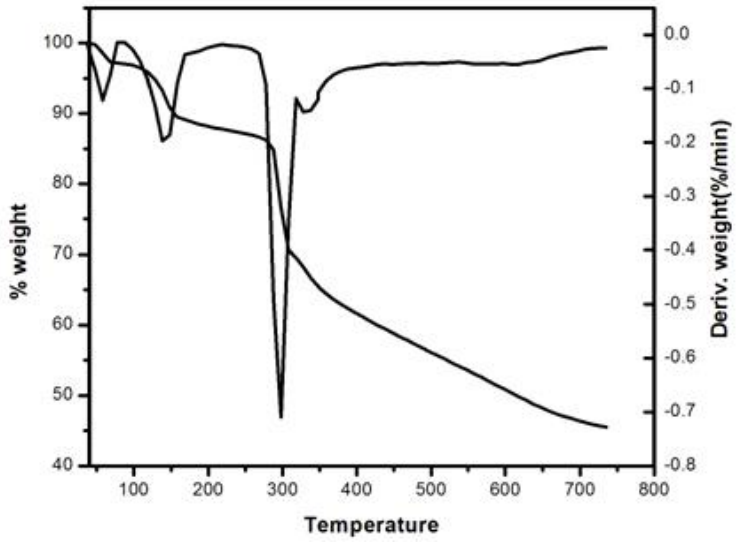

Fig. 3. The TG-DTG curves for the thermal degradation of rubrocurcumin

The mechanistic equations employed were based on the values of f (α) and g (α) which corresponds to different mechanism for solid state reactions (Vyazovkin and Wright, 1998) and are listed in Table 1. The other kinetic parameters ΔH, ΔS, and ΔG were calculated using the equations (11), (12) and (13) (Asadi *et al*., 2015).

$$\Delta\mathrm{H} = \mathrm{Ea} - \mathrm{RT} \quad \ldots (11)$$

$$\Delta\mathrm{S} = \mathrm{R}\left[\ln\left(\frac{\mathrm{Ah}}{\mathrm{kT}}\right) - 1\right] \quad \ldots (12)$$

$$\Delta\mathrm{G} = \Delta\mathrm{H} - \mathrm{T}\Delta\mathrm{S} \quad \ldots (13)$$

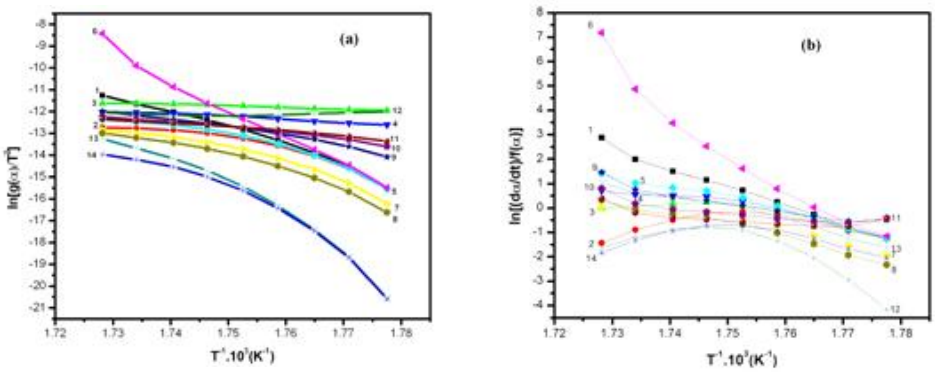

Fig. 4. Plot of ln[(g(α)/T^2]vs. 1/T (a) and ln[(dα/dt)/f(α)]vs. 1/T (b) using 14 different solid state reaction models for the second degradation stage.

Results and discussion

The structure of rubrocurcumin was confirmed by comparison of UV, IR, NMR and MS data with literature (Sui *et al.*, 1993, Vijayalakshmi *et al.*, 1981). The TG-DTG curves for the thermal degradation of rubrocurcumin are shown in Fig. 3. The obtained data indicate that the thermal degradation of rubrocurcumin follows four distinct stages. First degradation stage is due to the removal of hydrogen bonded water molecule. Thermal degradation of the compound starts only at 287°C, indicating its high thermal stability.

An initial 2.37% weight loss was observed at 65°C, which may be due to the presence of moisture and trapped solvents (Gao *et al*, 2004). The first decomposition stage was observed in the range 110-148°C with a mass loss (Calcd./Found%;7.39, 7.72%) assigned to the loss of two hydrogen bonded water molecule. A similar water loss is reported for the curcumin metal complexes in this temperature range (Refat, 2013). The second stage was observed in the temperature range 287-305°C, ascribed to the loss of oxalate group equivalent to a mass loss of C_2O_3 (CO-CO-O) molecule. (Calcd./Found%; 18.88, 19.12%). In the third stage decomposition from 305-377°C a mass loss of 7.29% was observed (Calcd./Found%; 7.29, 7.40) which corresponds to the loss of two OH groups present in the benzene ring of curcumin moiety. These three stages are followed by a continuous degradation step from 377 - 750°C due to the decomposition of remaining part of curcumin (Refat, 2013, Chen et al., 2014). End product of thermal decomposition may be boric oxide.

The present group reported an increased thermal stability of transition metal complexes of curcumin (Priya *et al*., 2015) where the decomposition of curcumin moiety begins around 380-400°C and after 400°C there is complete decomposition (Zebib *et al*., 2010). The thermal degradation of curcumin moiety in rubrocurcumin also starts at high temperature (305°C) whereas the pure curcumin degrades after 190°C. Here we analyzed the mechanism and kinetics of thermal degradation of only the first two stages rubrocurcumin, since that of curcumin was reported previously (Chen *et al*., 2014).

The fractional reaction versus time graphs for the water decomposition and oxalate decomposition stages of rubrocurcumin are analyzed by linear regression method by the fourteen heterogeneous solid state reactions listed in Table 1. The function f (α) and g (α) are substituted in equation (3) and (10) and the plots were drawn using ln (g(α)/T^2) vs. 1/T for equations (3) and ln [(dα/dt)/f (α)] vs. 1/T for equation (10) and are given in Fig 4. The Ea and

A is determined from slope and intercept of these plots and are listed in Table 2. Out of the fourteen solid state reaction models which gives better correlation coefficient (R^2) nearer to one and the values of Ea and A obtained by those methods were approximately equal, that was the probable thermal decomposition mechanism of the complex.

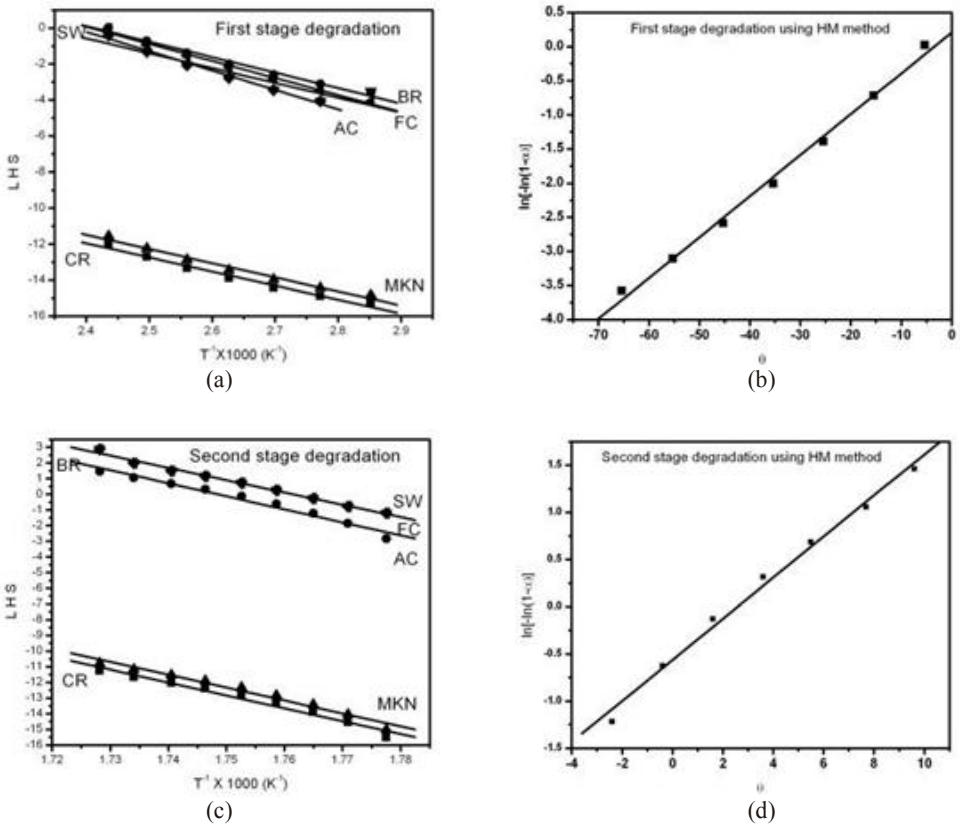

Fig. 5. CR, BR, MKN, SW, AC and FC plots for the first (a) and second (c) degradation stages, HM plot for the first (b) and second (d) degradation stage of rubrocurcumin

The correlation using CR and AC method failed in predicting correct model for the first degradation stage of rubrocurcumin. All the models seem to be better fit for this stage using AC method but CR method indicates first and fifth models are better. By comparing Ea and A values of first and fifth models we come to a conclusion that first model fits better to this stage. The unpredictability of correct model for this stage may be due to the removal of hydrogen bonded fragment.

Mampel equation for first order reaction gives maximum R^2 value and approximately equal Ea and A values for CR and AC method for the second stage degradation for rubrocurcumin. Thus, it may be concluded that the first order Mampel power law for a chemical reaction process fits to the degradation process of rubrocurcumin.

The thermal stability of rubrocurcumin are analyzed in terms of decomposition kinetic parameters derived from the first order thermal degradation kinetic equation based on CR, BR, MKN, HM, FC, SW and AC method. Representative computerized plots are given in Fig. 5. Each plot gave a straight line showing the order of the reaction as unity. The correlation coefficient (R^2) of the linearization plots of the thermal decomposition steps, using seven

calculation methods, are found to lie in the range 0.983 to 0.996, showing a good fit with the linear function which also indicate the reaction order as unity.

The kinetic parameters Ea, A, ΔH, ΔS and ΔG calculated for the thermal degradation of rubrocurcumin using the non-mechanistic methods are summarized in Table 3. There is considerable variation in the calculated kinetic parameters especially for ΔS. So we come to a conclusion that the actual values of the kinetic parameters corresponding to thermal degradation depend not only on factors like atmosphere, sample size, sample mass and heating rate but also depends upon the mathematical treatment used for the evaluation of the data.

The activation energy calculated using different methods are positive indicating that no phase transition took place in the selected temperature range (Ramukutty *et al*., 2014). High value of frequency factor, A for the second stage, indicates that the decomposition reaction follows a fast reaction (Zhao *et al*., 2003). The positive values of ΔH mean that the two decomposition stages are endothermic. The negative value of ΔS for the first degradation step shows more ordered structure for the activated complex than the reactants, and the reactions are slower than the normal. ΔS for the second stage is positive, which indicate the irreversible nature of the degradation. The positive value of ΔG shows that the reaction involved in the decomposition of rubrocurcumin is not spontaneous.

Conclusion

Rubrocurcumin was synthesized in pure form and its structure was confirmed by different spectral techniques. It was found that the thermal decomposition of rubrocurcumin occurred in four distinct stages and the main pyrolysis process occurred in the temperature range 287-305°C, due to the degradation of oxalate group. Fractional reaction – time graph according to different solid state reaction model find out the mechanism of decomposition for this stage as Mampel equation of first order kinetics. Thermal decomposition behaviour and various kinetic parameters were evaluated using seven different non-mechanistic methods. Kinetic studies reveal that there is considerable variation in the calculated kinetic parameters. Abnormally high value of frequency factor for the second stage indicates this step as a fast reaction. Fairly straight line plots obtained for all the seven methods also indicates first order kinetics for degradation.

Acknowledgements

The authors are thankful to the SAIF, CUSAT for carrying out the spectral analysis. One of the authors (JJ) is grateful to CSIR for the financial support in the form Senior Research Fellowship.

References

1. Achar, B.N.N., Bridley, G.W. and Sharp, J.H., *Proceeding of Int. Clay Conference, Jerusalen*, **1**, 67 (1966).
2. Asadi, M., Asadi, Z., Savaripoor, N., Dusek, M., Eigner, V., Shorkaei, M.R. and Sedaghat, M., *Spectrochimica Acta Part A : Mol. and Biomol. Spectroscopy*, **136**, 625 (2015).
3. Asha, R., Devi, R.S. Priya, R.S., Balachandran, S., Mohanan, P.V. and Abraham, A., *Chem. Biol. Drug Des*., **80**, 887 (2012).
4. Baker, A.S., *Agric Food Chem*., **12**, 4 (1964).
5. Balaban, A.T., Parkanyi, C., Ghiviriga, I., Aaron, J., Zajickova, Z.B.E. and Martinez, O.R., *Arkivoc,* **13**, 1 (2008).

6. Balogun, A.O., Lasode, O.A. and McDonald, A.G., *Bioresour. Technol.,* **156**, 57 (2014).
7. Borsari, M., Ferrari, E. Grandi, R. and Saladini, M., *Inorganica Chimica Acta*, **328**, 61 (2002).
8. Broido, A.A., *J. Polym. Sci.,* **2A**, 1761 (1969).
9. Chen, Z., Xia, Y., Liao, S., Huang, Y., Li, Y., Hea, Y., Tong, Z. and Li, B., *Food Chem.*, **155**, 81 (2014).
10. Coats, A.W. and Redfern, J.P., *Nature,* **201**, 67 (1964).
11. Deodhar, S.D., Sethi, R. and Srimal, R.C., *Indian Med. Res.,* **71**, 632 (1980).
12. Flynn, J.H., *J. Therm. Anal*., **27**, 95 (1983).
13. Freeman, E.S. and Carroll, B., *J. Chem. Rev.,* **62**, 394 (1958).
14. Gao, J., Xia, L. and Liu, Y., *Polym. Degrad. Stab.,* **83**, 71 (2004).
15. Henriquea, M.A., Netoa, W.P.F., Silvérioa, H.A., Martinsa, D.F., Gurgel, L.V.A., Barud, H.S., Carlos De Morais, L. and Pasquini, D., *Ind. Crops Prod.,* **76**, 128 (2015).
16. Horowitz, H.H. and Metzger, G., *Anal. Chem.*, **35**, 1465 (1963).
17. Jordan, W.C. and Drew, C.R., *J. Natl. Med. Assoc.,* **88**, 333 (1996).
18. Katherine, L., Stephen, E.F., Gabriele, K., Christopher, G.F. and Tony, D.J., *Anal. Methods,* **4**, 2215 (2012).
19. Kurien, B.T. and Scofield, R.H., *Trends Pharmacol. Sci*., **30**, 334 (2009).
20. Kuttan, R., Bhanumathy, P. Nirmala, K. and George, M.C., *Cancer Lett*., 29 (1985).
21. Madhusudhanan, P.M., Krishnan, K. and Ninan, K.N., *Thermochim Acta*, **97**, 189 (1986).
22. Mair, J.W and Day, H.G., *Anal. Chem.,* **44**, 12 (1972).
23. Priya, R.S., Balachandran, S., Daisy, J. and Mohanan, P.V., *Univ. J. of Phys. and Appl*., **3**, 6 (2015).
24. Priyadarsini, K.I., *Molecules*, **19**, 20091 (2014).
25. Ramajo-Escalera, B., Espina, A., García, J.R., Sosa-Arnao, J.H. and Nebra, A.S., *Thermochim. Acta,* **448**, 111 (2006).
26. Ramukutty, S. and Ramachandran, E., *J. Cryst. Process Technol*., **4**, 71 (2014).
27. Refat, M.S., *Spectrochimica Acta Part A : Mol. and Biomol. Spectroscopy,* **105**, 326 (2013).
28. Sharma, O.P., *Biochem. Pharmacol.,* 25, 1811 (1976).
29. Sharp, J.B. and Wentworth, S.A., *Anal. Chem*., **41**, 2060 (1969).
30. Srimal, R.C. and Dhawan, B.N., *J. Pharm. Pharmaco.,* **25**, 447 (1973).
31. Sui, Z. Salto, R., Li, J., Craik, C. and Ortiz de Montellano, P.R., *Bioorg. Med. Chem*., **1**, 415 (1993).
32. Vijayalaksmi, R., Sathyanarayana, M.N. and Rao, M.V.L., *Ind. J. Chem*., **20B**, 907 (1981).
33. Vyazovkin, S.G. and Wight, C.A., *Int. Rev. Phys. Chem*., **7**, 407 (1998).
34. Zebib, B., Mouloungui, Z. and Noirot, V., *Bioinorg. Chem. Appl.,* **2010**, 1 (2010).
35. Zhao, H., Wang, Y. Z., Wang, D.Y., Wang, B., Wu, B. and Clen, D.Q., *Polym. Degrad. Stab*., **80**, 135 (2003).

❑